Optimal Operation of Industrial Energy Hubs in Smart Grids

Sumit Paudyal, *Member, IEEE,* Claudio A. Cañizares, *Fellow, IEEE,* and Kankar Bhattacharya, *Senior Member, IEEE*

***Abstract*—This paper presents the development of a generic optimal industrial load management (OILM) model, which can be readily incorporated into Energy Hub Management Systems (EHMSs) for industrial customers, in interaction with local distribution companies (LDCs), for automated and optimal scheduling of their processes. The mathematical models comprise an objective function to minimize the total energy costs and/or demand charges for industrial customers, and a set of equality and inequality constraints to represent the industrial process, storage units, distribution system components, operator's requirements, and other relevant constraints. The effectiveness of the proposed OILM model is demonstrated in two industrial customers: a flour mill and a water pumping facility. The results show that the proposed OILM model, in conjunction with communication and control infrastructures at the customer and LDC levels, would allow optimal operation of industrial EHMSs in smart grids.**

***Index Terms*—Distribution systems, industrial load management, energy management systems, optimization.**

I. Nomenclature

Parameters:

$a_0 - a_{11}$	Coefficients of function $f(\cdot)$.
C	Total number of storage units.
ΔT	Duration of an interval in hr.
D	Down-time of industrial process in hr.
DP	Process inter-dependency matrix.
E	Total number of measurements.
GP	Gaps between processes in hour.
I_{max}	Maximum material inflow rate per hour.
I_{min}	Minimum material inflow rate per hour.
J	Total number of industrial processes.
λ	Peak demand charge in \$/kW/month prorated per day.
L_0	Initial storage level.
L_{cap}	Storage capacity.
L_{min}	Minimum allowed storage level.
L_{req}	Required storage level.
M	Total number of input variables.
N	Total number of output variables.
O_{max}	Maximum material outflow rate per hour.
O_{min}	Minimum material outflow rate per hour.
P_{max}	Peak demand requirement set by an LDC.
ρ	Energy price in \$/kWh.
R	Process I/O matrix.
T	Total number of intervals.
T_1	First interval of scheduling window.
T_2	Last interval of scheduling window.
U	Up-time of industrial processes in hr.
V_{max}	Maximum voltage limit as per standard in kV.
V_{min}	Minimum voltage limit as per standard in kV.
Y_{max}	Maximum limits on non-electrical variables.
Y_{min}	Minimum limits on non-electrical variables.

Indices:

c	Storage unit number $1, 2, ..., C$.
cf	Storage unit number in which final products are stored $cf \in c$.
e	Number of measurement $1, 2, ..., E$.
j, k	Industrial process number $1, 2, ..., J$.
m	Input variable number $1, 2, ..., M$.
n	Output variable number $1, 2, ..., N$.
τ, t	Time interval $1, 2, ..., T$.
tf	Time interval for which the requirements of final products are set $tf \in t$.

Variables:

ε	Positive slack variable.
i	Input flow rates per hr.
l	Storage level.
o	Output flow rates per hr.
p	Total power consumption in kW.
pd	Active power demand in kW.
$\tilde{pd}$	Measured active power demand in kW.
$\hat{pd}$	Estimated active power demand in kW.
p_{peak}	Auxiliary variable to model peak demand.
Q	Water discharge rate of the pumps in m^3/hr.
$\tilde{Q}$	Measured water discharge rate of the pumps in m^3/hr.
$\hat{Q}$	Estimated water discharge rate of the pumps in m^3/hr.
Qd	Reactive power demand of processes or storage units in kvar.
r	Auxiliary variable to calculate total number of ON decisions for a process.
s	Process ON/OFF status (1 ON, 0 OFF).
u	Decision to turn ON a process (1 ON).
v	Decision to turn OFF a process (1 OFF).
V	Average of applied three-phase voltage in kV.
w	Auxiliary variable.
y	Vector of non-electrical variables required

S. Paudyal is with the Department of Electrical and Computer Engineering, Michigan Technological University, Houghton, MI, USA (e-mail: sumitp@mtu.edu)

C. A. Cañizares and K. Bhattacharya are with the Department of Electrical and Computer Engineering, University of Waterloo, Waterloo, Ontario, Canada (e-mail: ccanizar@uwaterloo.ca; kankar@uwaterloo.ca).

to model processes or storage units.
Z Objective function.

Function:
$f(\cdot)$ Load estimation polynomial function to estimate active power demand.

II. Introduction

THE IMPLEMENTATION of real-time information systems, Advanced Metering Infrastructure (AMI), improved communication capabilities, and improved infrastructure for control systems is envisaged to transform the existing distribution systems into "Smart Grids". Similarly, at the customers' end, technologies such as smart meters, home/building automation, and industrial process automation render the electrical loads more manageable, controllable, and responsive to external signals, thus becoming an integral part of a smart grid [1]–[8]. In conventional distribution grids, energy management programs such as Demand Side Management (DSM), Demand Response (DR) and Demand Control (DC) are mostly implemented for aggregated loads or specific loads due to the lack of necessary infrastructure to manage individual loads. The infrastructure in smart distribution grids facilitate the realization of Energy Hub Management Systems (EHMSs) at customers' premises. An energy hub is defined as a node in an electric power system in which exchange of energy and information with energy sources, loads, and the external system take place [9]–[11]. Thus, the EHMS is a novel concept in smart grids concentrating on the real-time management of energy production, consumption, and storage at the customer level for the benefit of both customers and local distribution companies (LDCs) [12], [13].

The energy hub can range from aggregation of loads and energy sources at customer level to the aggregation of cluster of customers and DERs [9]–[11]. Thus, in [12], mathematical models required for the EHMSs for residential customers are proposed, which yield optimal operational decisions on scheduling their major loads to achieve one of the desired objectives related to energy cost, emissions, and comfort. In [14]–[16], mathematical models of various residential loads and energy sources are proposed in a similar context. This paper proposes a similar general approach as [12], with an emphasis on mathematical models required for industrial EHMSs.

Figure 1 presents the proposed schematic of an industrial customer's EHMS and its integration with the distribution grid as part of a smart grid. The proposed EHMS configuration consists of two main components: a central hub controller and an optimization engine. It is assumed that real-time information systems and communication infrastructure in smart grids allow the central hub controller access to information such as energy price, emissions, and DR incentive signals from the market operator. The central hub controller is also assumed to receive information on the industrial processes and their operating preferences from an

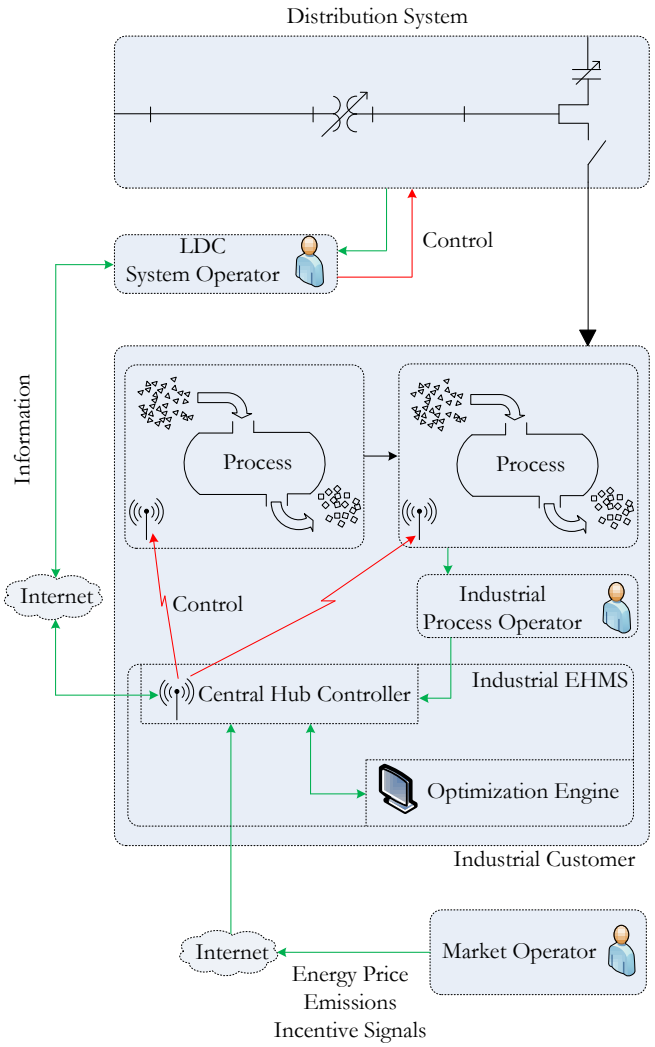


Fig. 1. Schematic of the industrial EHMS and external system.

industrial process operator, exchanging information such as aggregated load profiles with an LDC system operator for proper coordination with the corresponding distribution feeder operation and associated tap-changer and capacitor-bank controls. The optimization engine consists of the industrial load management model proposed in this work, and a solution method suitable for real-time applications. The information gathered by the central hub controller is then communicated to the optimization engine, which includes the system parameters and models required for load management, which in turn yields optimal schedules for the industrial processes to be relayed to the processes by the central hub controller for optimal dispatch purposes.

Most of the existing energy management activities focus on voltage optimization and load shifting at the aggregated load level [17]–[21]. Voltage optimization is a way of reducing power consumption of loads by varying the voltage within the limits prescribed by standards such as ANSI [22]. A Pacific Northwest study reveals that operating a distribution system in such a way can bring about 3% reduction in energy consumption [18]. In a separate study

carried out in [19] for an industrial customer (fiberboard production facility), it is demonstrated that voltage optimization can yield about 5% reduction in energy consumption. Similarly, load shifting activities are discussed in [20] and [21] in the context of aggregated load profiles for industrial customers, without considering the behavior of individual industrial processes and their interdependencies. The multi-objective optimization model for operational scheduling of water pumps proposed in [23], on the other hand, considers modeling of five independent centrifugal pumps. In [24], process dependencies in the modeling of a flour processing mill are presented, which, if generalized, can be applied to any process industry. In [25], the idea is extended to a petrochemical industry for optimal operation of a co-generation system considering the models of individual industrial processes. However, the mathematical models in [23]–[25] are very specific to the particular industry being modeled, where the industrial processes are simply represented by fixed active power loads independent of applied voltage and material flow rates, ignoring possible interaction with the distribution system operation and other process variables. In [26], active power demand of electric chillers and power generation of gas turbine are represented by functions of process variables; however, the process models are assumed to be independent of distribution system voltages.

Based on the aforementioned discussions, the main objective and contribution of present work is the development and validation of a generic Optimal Industrial Load Management (OILM) model, which can be readily incorporated into an EHMSs for any industrial customers, regardless of the nature of the processes. The proposed OILM model uses available distribution system information and control expected in smart grids, considering load control and voltage optimization approaches together. In this work, industrial process are represented by controllable loads that depend on variables such as material flow rates, applied voltage, and other relevant variables that can be controlled to modulate the customer's demand for the benefits of both the customers and the grid.

The rest of the paper is organized as follows: Section III describes the proposed OILM modeling, Section IV discusses the estimation of model parameters, Section V discusses the results of the case studies carried out for two industrial customers to demonstrate the application of the proposed model. The main contributions of the paper are highlighted in Section VI.

III. Mathematical Modeling

This section describes the set of equality/inequality constraints to represent industrial processes, storage units, distribution system components, operating limits, and other relevant components, plus the objective function that make up the proposed OILM model.

A. Industrial Processes

The industrial processes are modeled here as active and reactive power loads which depend on various controllable variables such as voltage, material flow rates, etc., representing the dynamics between ΔT intervals by modeling the process dependencies in time. However, the model does not capture the dynamics changing within an interval ΔT, assuming that the system remains unchanged during these intervals, thus modeling the load as a quasi-static process.

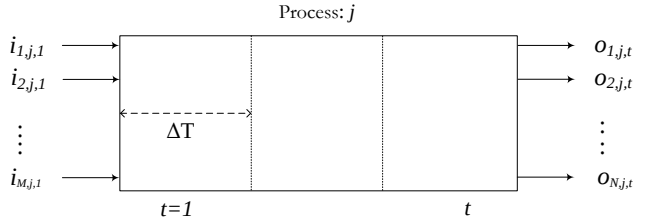


Fig. 2. Generic input/output model of a process.

1) Material Inflow/Outflow: Industrial loads can be modeled as processes, comprising one or multiple devices operating together, and can be considered as a multi-input, multi-output, multi-interval system, as shown in Fig. 2, where the input and output variables represent the rate of inflow and outflow of material respectively. For each industrial process j, a matrix R_j (referred here as process I/O matrix), relating the material inflow and outflow rates in each time interval, can be defined as follows:

$$\begin{bmatrix} o_{1,j,t} \\ o_{2,j,t} \\ \vdots \\ o_{N,j,t} \end{bmatrix} = \underbrace{\begin{bmatrix} R_{1,1,j} & R_{1,2,j} & .. & R_{1,M,j} \\ R_{2,1,j} & R_{2,2,j} & .. & R_{2,M,j} \\ \vdots & \vdots & .. & \vdots \\ R_{N,1,j} & R_{N,2,j} & .. & R_{N,M,j} \end{bmatrix}}_{\begin{bmatrix} R_j \end{bmatrix}} \begin{bmatrix} i_{1,j,t} \\ i_{2,j,t} \\ \vdots \\ i_{M,j,t} \end{bmatrix} \forall j, \forall t \quad (1)$$

All variables, parameters and indices in these and other equations are defined in Section I. Here, the R_j is a matrix of numbers, and its size depends on the number of input/output variables required to model the process. The R_j for an individual process can be determined from historical measurement and from the knowledge of the process, as explained in Section IV.

2) Process Interdependencies: The status (ON/OFF) of one process may or may not be governed by the status of another process; hence, a process interdependency model is developed to represent various scenarios. Such interdependencies can broadly be categorized into independent and dependent processes [24], [27], as explained next.

Independent Processes: The status of such processes are independent of other processes and can be scheduled at any time interval along a scheduling window ($T_{1,j}$ to $T_{2,j}$). The

following equations define an independent process j:

$$u_{j,t} + \sum_{\tau=t+1}^{t+U_j-1} v_{j,\tau} \leq 1 \qquad \forall j, T_{1,j} \leq t \leq T_{2,j} - U_j + 1 \quad (2a)$$

$$v_{j,t} + \sum_{\tau=t+1}^{t+D_j-1} u_{j,\tau} \leq 1 \qquad \forall j, T_{1,j} \leq t \leq T_{2,j} - D_j + 1 \quad (2b)$$

$$u_{j,t} + v_{j,t} \leq 1 \qquad \forall j, T_{1,j} \leq t \leq T_{2,j} \quad (2c)$$

$$u_{j,t} - v_{j,t} = s_{j,t} - s_{j,t-1} \qquad \forall j, T_{1,j} \leq t \leq T_{2,j} \quad (2d)$$

Equations (2a)-(2d) ensure that the minimum up-time and down-time requirements of the processes are satisfied.

Dependent Processes: The decision to change the status of dependent processes can be moved along a scheduling window, but their flexibility is limited by the status of other processes. For dependent processes, a parameter matrix DP is defined, and proper values are assigned to its elements to distinguish among various kinds of dependencies. In this work, three dependent processes are modeled as follows:

- *Sequential Processes ($DP_{j,k} = 1$ or 2)*: Two processes j and k are said to be sequential when the operation of k starts only after the operation of j is complete, and the sequence of operation is predefined, i.e., k follows j. The following equations are required to model two sequential processes j and k:

$$w_{j,t} = \sum_{\tau=1}^{t} u_{j,\tau} \qquad \forall j, \forall t \quad (3a)$$

$$w_{k,t} \leq w_{j,t} \qquad \forall j, \forall k : DP_{j,k} = 1 \vee 2, \forall t \quad (3b)$$

$$s_{j,t} + s_{k,t} \leq 1 \qquad \forall j, \forall k : DP_{j,k} = 1 \vee 2, \forall t \quad (3c)$$

  Equations (3a)-(3c) do not require processes j and k to operate for the same number of time intervals in the optimization horizon. Such sequential processes are distinguished from others by $DP_{j,k} = 2$, and modeled using the following additional equations:

$$r_j = \sum_{t} u_{j,t} \qquad \forall j \quad (4a)$$

$$r_j = r_k \qquad \forall j, \forall k : DP_{j,k} = 2 \quad (4b)$$

- *Interlocked Processes ($DP_{j,k} = 3$):* These processes are special cases of sequential processes in which there is a fixed time gap between the turning ON of the processes j and k. For interlocked processes, a parameter matrix GP is defined which contains the required time gaps. The following equation is required to model two interlocked processes j and k:

$$u_{k,t} = u_{j,t-GP_{j,k}} \qquad \forall j, \forall k : DP_{j,k} = 3, \forall t \quad (5a)$$

$$r_j = r_k \qquad \forall j, \forall k : DP_{j,k} = 3 \quad (5b)$$

- *Parallel Processes ($DP_{j,k} = 4$):* These processes are similar to the interlocked processes, but with no time gap between the turning ON of the processes j and k. The following equations are required to model two parallel processes j and k:

$$u_{j,t} = u_{k,t} \qquad \forall j, \forall k : DP_{j,k} = 4, \forall t \quad (6)$$

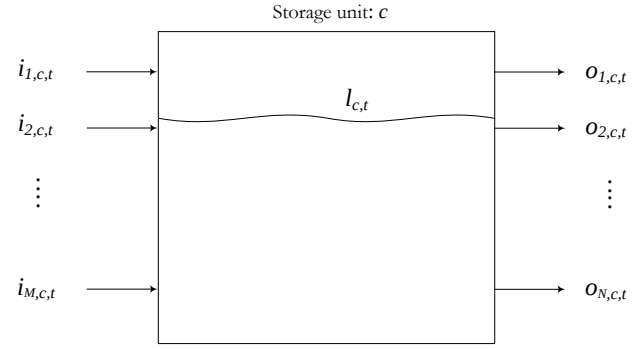


Fig. 3. A generic model of a storage unit.

B. Storage Units

Storage units are modeled as multi-input, multi-output systems as shown in Fig. 3. The following mathematical equations model a storage unit c:

$$L_{0,c} + \sum_{m} i_{m,c,t} - \sum_{n} o_{n,c,t} = l_{c,t} \qquad \forall c, t = 1 \quad (7a)$$

$$l_{c,t-1} + \sum_{m} i_{m,c,t} - \sum_{n} o_{n,c,t} = l_{c,t} \qquad \forall c, t \geq 2 \quad (7b)$$

Equation (7a) calculates the storage level for the first time interval in the optimization horizon based on the initial storage level, whereas (7b) calculates the storage level for subsequent time intervals.

C. Distribution System Components Model [28]

Distribution system components such as conductors/cables, transformers, Load Tap Changers (LTCs), and switches are modeled using ABCD parameters. Single-phase, two-phase, three-wire three-phase, and four-wire three-phase conductors and cables are also represented. Various common distribution system transformers are modeled, such as single-phase and three-phase wye grounded-wye grounded, delta-wye grounded, and open wye-open delta connections. Single-phase LTCs and wye-connected three-phase LTCs are modeled with individual phase control and group control options. Capacitors are modeled as constant impedance loads, and capacitor banks are modeled as multiple units of Switched Capacitors (SCs). The electrical loads in the distribution system are represented by variable active power and reactive power loads, as discussed next in Section III.D. A detailed mathematical model of the distribution system components are presented in [29], which are implemented in [28] in an optimization framework. Note that the load control approach does not require the modeling of distribution system components, but it is required if a voltage optimization approach is considered in the context of a smart grid.

D. Power Demand

For the OILM model considering both load control and voltage optimization, power demands correspond to the electrical active and reactive power consumed by the processes and storage units. Active power demands of

processes can be expressed in terms of input or output material flow rates, voltage, and other non-electrical control variables as follows:

$$pd_{j,t} = f_j(o_{n,j,t}, V_t, y_{j,t}) \qquad \forall j, \forall t \quad (8)$$

The polynomial functions $f(\cdot)$, referred here as load-estimation polynomial functions, can be determined from the knowledge of the processes/storage units and historical measurements. Similar equation, as (8), can be used to represent the active power consumed by the storage units. A detailed explanation on the estimation of these functions is presented in Section IV.

The total active power demand of the industrial loads at each time interval can be represented as the sum of the power demands of the processes and storage units; thus:

$$p_t = \sum_j pd_{j,t} + \sum_c pd_{c,t} \qquad \forall t \quad (9)$$

Observe that this equation considers only controllable loads; hence, it does not account for uncontrollable background loads such as lighting loads.

Similar equations, as (8) and (9), can be used to represent the reactive power consumptions. For an OILM model considering a load control approach only, the power demand can still be represented by (9) with the voltage fixed at its nominal value.

E. Peak Demand

Industrial customers are charged for peak demand since this is an important consideration for LDCs. Hence, there is a need to consider demand within the model to fully reflect the interaction of customers with LDCs in the context of a smart grid. Modeling of peak demand requires to find the maximum value of p_t ($\forall t$); which makes the optimization problem discontinuous. To avoid this, an auxiliary variable p_{peak} is minimized in the objective function, and used to constraint the peak demand as follows:

$$\lambda\, p_t \le \lambda\, p_{peak} \qquad \forall t \quad (10a)$$

$$\lambda\, p_{peak} \le \lambda\, P_{max} + \varepsilon \quad (10b)$$

These equations ensure that the demand in each interval is always less than or equal to the value of the auxiliary variable, which in turn should be less than a peak power demand P_{max} predefined by the LDC as part of a DR program, if applicable. Parameter λ is included on both sides of equations (10a) and (10b) to make the model generic, so that the model can be used for the minimization of energy charges and/or minimization of demand charges; thus, customers seeking to minimize the energy charges only can set $\lambda = 0$ in the model, thus eliminating equations (10a) and (10b). A slack variable ε is used in (10b) to prevent infeasible cases when the value of P_{max} set by the LDC is too low, and thus not achievable by the OILM model.

F. Limits on Process/Storage Variables

Each process can have limits on the input and output material flow rates and on the other non-electrical variables associated with it, which are modeled as follows:

$$I_{min,m}\, s_{j,t} \le i_{m,j,t} \le I_{max,m}\, s_{j,t} \qquad \forall m, \forall j, \forall t \quad (11a)$$

$$O_{min,n}\, s_{j,t} \le o_{n,j,t} \le O_{max,n}\, s_{j,t} \qquad \forall n, \forall j, \forall t \quad (11b)$$

$$Y_{min,j}\, s_{j,t} \le y_{j,t} \le Y_{max,j}\, s_{j,t} \qquad \forall j, \forall t \quad (11c)$$

When a process is ON ($s_{j,t} = 1$), the flows and all other electrical/non-electrical variables associated with it must be in a range defined by the minimum and maximum limits, and when the process is OFF ($s_{j,t} = 0$), all of them must be zero. Similarly, limits on storage level can be represented as:

$$L_{min,c} \le l_{c,t} \le L_{cap,c} \qquad \forall c, \forall t \quad (12)$$

G. Production Requirements

Production requirements are enforced in terms of cumulative levels of one or more storage units that contain final products at one or more time intervals in the optimization horizon. This can be represented as follows:

$$\sum_{cf} l_{cf,tf} \ge L_{req,tf} \qquad \forall tf \quad (13)$$

H. Optimization Objective

Given the importance of costs to industrial customers, the minimization of the customer's energy cost and peak demand charges is considered as the optimization objective. This can be represented as follows:

$$Z = \overbrace{\Delta T \sum_t \rho_t\, p_t}^{\text{Energy costs}} + \overbrace{\lambda\, p_{peak}}^{\text{Peak demand charges}} \quad (14)$$

This objective function can also be used for an industrial customer that chooses to minimize its energy costs or peak demand charges only, by setting $\lambda = 0$ or $\rho_t = 0$, respectively.

Equations (1)-(13) represent the equality and inequality constraints, which along with (14) form the OILM model. Note that other inequality constraints representing limits on processes variables and distribution system operational requirements, such as voltage, feeder current, and material flow limits, can be readily incorporated into the proposed OILM model. Depending on the order of the load-estimation polynomial functions, the OILM model can be either a mixed integer linear programming (MILP) or a mixed integer non-linear programming (MINLP) problem, as demonstrated in the case studies in Section V.

IV. Model Parameter Estimations

This section explains the estimation of process I/O matrices used in (1), and load-estimation polynomial functions used in (8). Note that other model parameters used in (1)-(14) are straightforward to obtain and are provided in the Appendix for the case studies discussed in Section V.

A. Process I/O Matrix

As explained in Section III, the process I/O matrices relate the material inflow and outflow rates in each time interval.

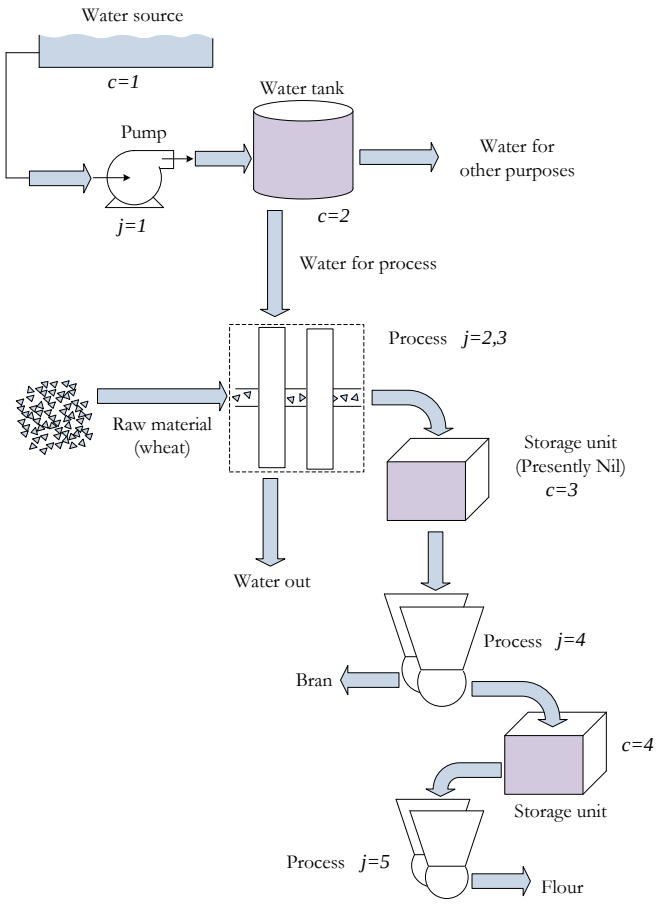


Fig. 4. Schematic diagram of a flour mill showing the required processes and storage units [24].

Thus, consider the wheat bran removing machine, which is one of the processes used in the flour mill example discussed in Section V (Process $j = 4$ in Fig. 4). The input to the process is inflow rate of refined wheat, while the outputs are the outflow rates of bran and skinless wheat. From one set of measurements, the relation between inflow and outflow rates can be determined; thus, for example, if a certain amount of input wheat yields 80% of skinless wheat and 20% bran, the process input/output relation for the bran removing machine would be:

$$\begin{bmatrix} o_{1,t} \\ o_{2,t} \end{bmatrix} = \underbrace{\begin{bmatrix} 0.8 \\ 0.2 \end{bmatrix}}_{\begin{bmatrix} R \end{bmatrix}} \begin{bmatrix} i_{1,t} \end{bmatrix} \qquad \forall t \quad (15)$$

B. Load-estimation Polynomial Functions

Load-estimation polynomial functions model the relationship between the electrical active and reactive power demands with the electrical and non-electrical control variables associated with the processes. The estimation can be carried out either from knowledge of the process or from a least square error estimation of historical measurement data; the latter is explained in details next.

Consider a water pump, which is similar to one of the pumps used in the water pumping facility example described in Section V (Fig. 5). In this case, the electrical variable (voltage) and non-electrical variable (water discharge) are considered as input control variables, and the active and reactive power demands (outputs) are estimated using equations similar to (8). The estimation of the polynomial $f(\cdot)$ can be carried out based on available measurement data as follows: Assume e number of measurements are available for active power demand $\tilde{pd}_e$, voltage $\tilde{v}_e$, and discharge $\tilde{Q}_e$. Assume as well that polynomial $f(\cdot)$ is a quadratic function in $\tilde{v}_e$ and $\tilde{Q}_e$, which properly fits the available data based on a statistical analysis of the root mean square error; this analysis may yield higher degree polynomial depending on the process [31]. The estimated value of $\tilde{pd}_e$, given by $\hat{pd}_e$, can be obtained from the measurements of $\tilde{v}_e$ and $\tilde{Q}_e$ as follows:

$$\hat{pd}_e = f(\tilde{Q}_e, \tilde{v}_e) = a_0 + a_{01}\,\tilde{v}_e + a_{10}\,\tilde{Q}_e + a_{02}\,\tilde{v}_e^2 + a_{20}\,\tilde{Q}_e^2 + a_{11}\,\tilde{v}_e\,\tilde{Q}_e \qquad \forall e \quad (16)$$

Based on (16) and $\tilde{pd}_e$, the parameters a_0 to a_{11} of the polynomial $f(\cdot)$ are estimated using a least square error method, which can be modeled as an optimization problem as follows:

$$\text{Min.} \quad \sqrt{\frac{1}{E}\sum_e \left(\hat{pd}_e - \tilde{pd}_e\right)^2}$$

$$\text{s.t.} \quad \hat{pd}_e = f(\tilde{Q}_e, \tilde{v}_e) = a_0 + a_{01}\,\tilde{v}_e + a_{10}\,\tilde{Q}_e + a_{02}\,\tilde{v}_e^2 + a_{20}\,\tilde{Q}_e^2 + a_{11}\,\tilde{v}_e\,\tilde{Q}_e \quad \forall e \quad (17)$$

A similar procedure can be applied to estimate the parameters of the reactive power demand polynomial function.

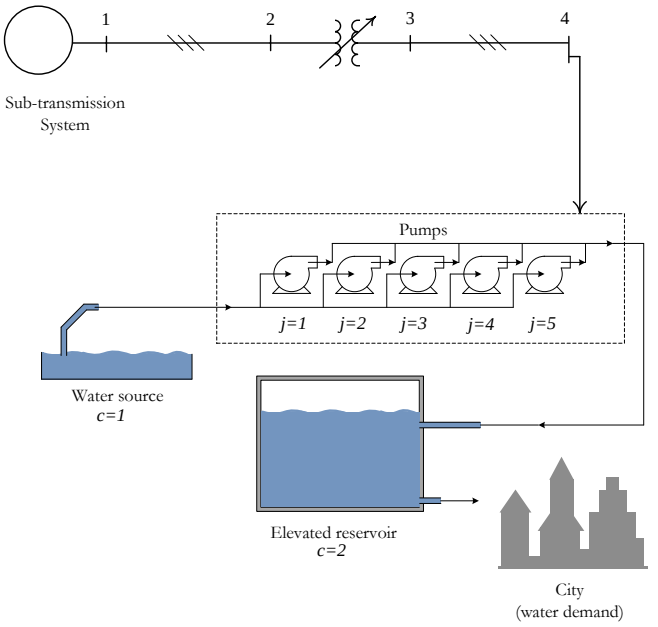


Fig. 5. Schematic diagram of a water pumping facility with processes and storage units [23], connected to the IEEE 4-node test feeder [30].

V. Case Studies

In this section, the OILM model proposed in Section III is applied to two industrial customers: a flour mill and a water

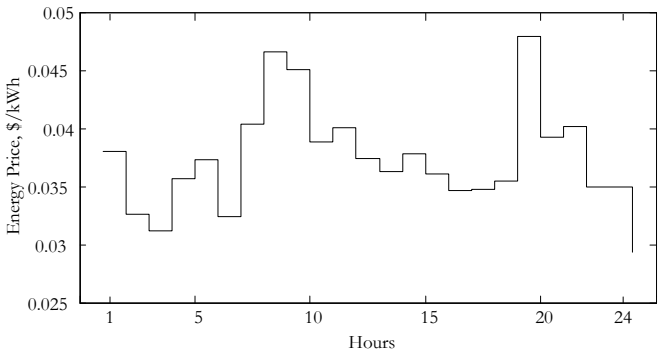


Fig. 6. HOEP on October 12, 2011 [34] .

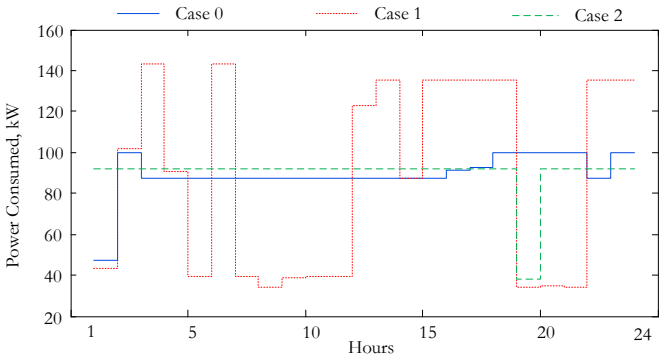


Fig. 7. Optimal operation of a flour mill.

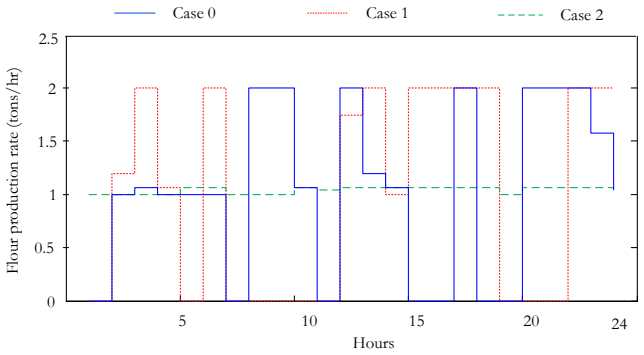


Fig. 8. Flour production rate.

pumping facility. The proposed models are developed in GAMS [32], a high-level optimization problem modeling tool, and solved using the KNITRO solver [33].

A. *Flour Mill Load Control*

The flour mill depicted in Fig. 4 is considered here [24]. It consists of 5 processes and 4 storage units. Process 1 is a pump to elevate water from a source to a storage tank. Process 2 and 3 represent washing and drying of raw material (wheat). Process 4 involves removal of bran from wheat, and process 5 is a grinding machine to produce flour. Information on the distribution system supplying power to the flour mill is not available, and hence the corresponding OILM model represents the load control approach only.

The only controllable variables in the flour mill facility are material outflow rates; the power demands to the processes are expressed in these terms. The processes are modeled as active power loads and the corresponding $f(\cdot)$ estimations are carried out from the knowledge of the processes. In the estimation process it is assumed that the rated electrical power of the 5 processes are 8 kW, 22 kW, 12.75 kW, 36.5 kW, and 78 kW, respectively [24]. Since no detailed information is available regarding the processes, the active power consumed by each processes is arbitrarily and without loss of generality assumed here to vary linearly with the outflow rate, and the process efficiency is assumed not to vary with the change in outflow rates. The coefficients of the linear polynomials $f(\cdot)$ thus obtained are provided in the Appendix.

For the simulation studies, the Hourly Ontario Electricity Price (HOEP) for October 12, 2011 is used as the energy price (Fig. 6) [34], as per real time pricing of industrial loads in Ontario, and $7/kW/month is used as the demand charge, which is the demand charge in Ontario during the fall [35]. The production requirement is considered to be 25 tons of flour per day. The minimum outflow rates for each process, when the process is ON, are assumed to be 50% of the outflow rates at rated power. The various other parameters required for the modeling of the processes and storage units are given in the Appendix.

Simulations are carried out for three different cases and the results are summarized in Table I. Case 0 is a base case that is used for comparison purposes and corresponds to a non-optimized energy consumption profile of an industrial customer, which is basically a feasible solution of the OILM model, i.e., a solution that satisfies all equality and inequality constraints of the model. Case 1 corresponds to minimization of energy costs, and Case 2 corresponds to minimization of both energy costs and demand charges. Observe in Table I that the developed OILM yields a ~5% reduction in energy costs and a ~2.8% reduction in total costs (highlighted in the table). However, these figures depend on various factors such as limits on the material flows, variation on process efficiencies with the out-flow rates, initial storage levels, flexibility in scheduling of the processes, energy prices, and demand charges.

TABLE I
PERFORMANCE OF OILM FOR A FLOUR MILL

		Case 0	Case 1	Case 2
Energy Costs [$/day]		80.81	76.50	79.76
Demand Charges† [$/day]		23.28	33.48	21.42
Total Costs [$/day]		104.09	109.98	101.18
Energy [kWh/day]		2164.70	2149.42	2149.42
Peak Demand [kW]		99.76	143.48	91.80
% Difference w.r.t. Case 0	Energy Costs	—	-5.33	-1.30
	Demand Charges	—	43.82	-7.98
	Total Costs	—	5.66	-2.79
	Energy	—	-0.71	-0.71
	Peak Demand	—	43.82	-7.98

† Monthly charges prorated per day.

The 24-hour power consumption profiles and flour production rate of the three cases are shown in Fig. 7 and Fig. 8, respectively. Case 1 results in minimum energy cost and is 5.3% less compared to Case 0. Note that the power consumption profile for Case 1 complies with the HOEP, i.e., the electricity price is low at hours 3, 6, 16, and 24, resulting in an increased power consumption at these hours; as a consequence, the peak demand is increased by 43.8% compared to Case 0 (this shifted peak demand increase has been observed in [12] as well). In Case 2, both energy costs and demand charges are less as compared to Case 0; the reduction in demand charges is 7.9% compared to Case 0, while the reduction is energy costs is 1.3%. Due to the maximum flexibility assumed in terms of personnel schedules and programs during the operating hours (i.e., 24 hours), since only automatic processes are considered, the resulting power profiles for Case 2 are nearly flat, thus reflecting only economic and technical objectives. The difference in the energy required for the base case and the optimized cases can be attributed to the difference in storage levels at the end of the optimization horizon. The energy consumptions in Case 1 and Case 2 are the same due to the fact that the same final storage levels are obtained in both cases, and due to the assumed constant efficiency of the processes.

B. Water Pumping Facility Load Control and Voltage Optimization

The water pumping facility considered here is depicted in Fig. 5 [23], and consists of 5 processes and 2 storage units. Processes 1 through 5 are centrifugal pumps which elevate water from a source to a reservoir. The rated electrical power of Processes 1, 2 and 3 are 595 kW, 445 kW, and 260 kW, respectively; Process 5 is identical to Process 1; and Process 4 is identical to Process 2. The water pumping facility is assumed to be connected to the end of the IEEE 4-node test feeder [30], as depicted in Fig. 5, to demonstrate the combined effect of load control and voltage optimization in the OILM model discussed in Section III. The voltage in the IEEE 4-node test feeder is controlled by an LTC equipped transformer. Hence, the control variables are the LTC position which controls the voltage applied to the pumps and the pumps' water discharge rates. In this case study, the IEEE 4-node test system is considered for illustration purposes only; the optimal operation of distribution feeders from the LDC operator's perspective of practical sized distribution systems is discussed in detail in [28].

Because of the lack of historical measurement data in this case, data were generated using detailed PSCAD simulations [36]. In these simulations, the pumps were assumed to be connected to a three-phase voltage source with nominal voltage of 4.16 kV, and multiple studies were carried out by varying the voltage from 0.95 p.u. to 1.05 p.u., and the speed from 0.97 p.u. to 0.999 p.u. The recorded data from the simulations and pump performance curves are then used to estimate quadratic load-estimation polynomials as discussed in Section IV.B; the coefficients thus obtained are given in the Appendix.

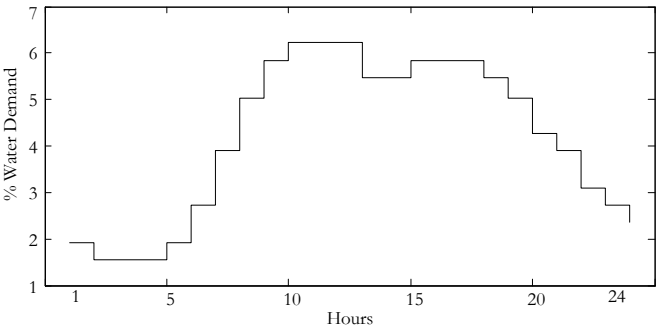


Fig. 9. City water demand profile for 24-hours [23].

Similar to the previous studies, the HOEP for October 12, 2011 is considered as the energy price (Fig. 6) [34], and \$7/kW/month is used as the demand charge [35]. The production requirement in this case is the 24-hour water demand profile shown in Fig. 9, and the total water required for the city in 24 hours is assumed to be 54,788 m^3, as per [23]. The minimum outflow rates for each process, when the process is ON are assumed to be 50% of the outflow rates at the rated power. The various other parameters required for the modeling of the processes and storage units are provided in the Appendix.

Simulations are carried out for three different cases and the results are summarized in Table II; the 24-hour power consumption profiles obtained for the three cases are shown in Fig. 10. Similar to the previous studies, Case 0 corresponds to a non-optimized, feasible base case; Case 1 corresponds to minimization of energy costs; and Case 2 corresponds to minimization of both energy costs and demand charges. Case 1 results in a 38.1% reduction in energy costs as compared to Case 0 as highlighted in the table, but a 73.7% increase in peak demand, which is consistent with the results obtained for the Flour Mill. In Case 2, both the energy costs and demand charges are less as compared to Case 0, the reductions are 25.0% and 63.6%, respectively, and results in 38.1% savings on the total costs as highlighted in the table. Note that these numerical figures depend on various factors such as limits on the material flows, variation of process efficiencies with out-flow rates, initial storage levels, flexibility in scheduling of the processes, energy prices, and demand charges. As in the case of the flour mill, the resulting flat load profile in Case 2 is due to the maximum flexibility assumed in terms of personnel schedules and programs in the scheduling of the processes during the operating hours (i.e., 24 hours). The difference in energy required for the three cases can be attributed to the difference in optimal storage level profiles, and changes in the efficiencies of the processes as the water discharge rate and voltage vary.

Another set of case studies were also carried out considering only load control, to compare the savings with those obtained with voltage optimization. In this case, only an estimation of the polynomials to represent active powers is required, which

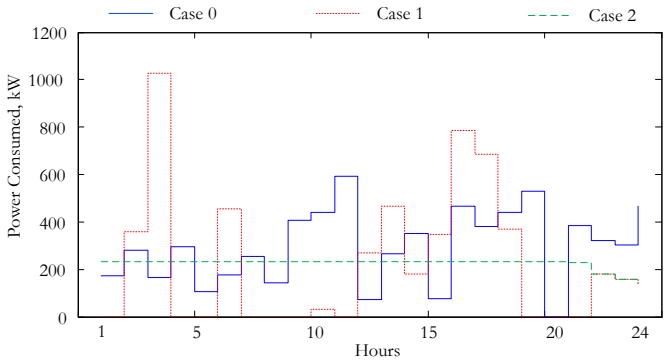


Fig. 10. Optimal operation of a water pumping facility connected to the IEEE 4-node test feeder.

is readily obtained by fixing the voltage at its nominal value in the load-estimation polynomials provided in the Appendix. Thus, the only controllable variables in the system are the water discharge rates of the pumps. In these studies, a base case, i.e. Case 0, is not relevant, since the objective here is to determine the possible savings accrued by means of the voltage optimization approach.

The results of these case studies are summarized in Table III, along with a comparison with the corresponding voltage optimization cases in Table II. Observe that the energy costs increase by 13.2% in Case 1, and total cost increase by 1.7% in Case 2, as highlighted in the table. These figures demonstrate that the voltage optimization approach yields additional savings for industrial customers, and is consistent with the savings reported in [18] and [19].

C. Computational and Implementation Considerations

In the case studies presented in this section, consideration of pro-rated peak demand charges is just an approximation, as peak-demand is charged based on power consumption profiles over a billing cycle. Thus, the assumption made here is that the load behavior of the industrial customer for the day considered yields the highest peak demand compared to other days in the billing cycle.

For the flour mill system, the number of continuous variables, integer variables, and constraints are 795, 388, and 7861, respectively, resulting in OILM solution times of less than 3.5 minutes. For the water pumping facility and associated distribution feeder, the number of continuous and integer variables are 3,243 and 557, respectively, and the total number of constraints are 10,794, yielding solution times of less than 5 minutes. Considering that the proposed OILM model incorporates distribution system components and industrial load models, real-time operation would include the optimization model solution and the dissemination of the necessary control signals to the corresponding equipment in the distribution feeder and processes at the industrial facility. Given the large number of nodes and components encountered in practical feeders and industrial facilities, this would result in significant data handling and computational burdens, thus making real-time continuous control infeasible. Hence, in this case, a practical

TABLE II
PERFORMANCE OF OILM FOR A WATER PUMPING FACILITY CONNECTED TO THE IEEE 4-NODE TEST FEEDER.

		Case 0	Case 1	Case 2
Energy Costs [$/day]		266.65	165.08	200.08
Demand Charges† [$/day]		137.91	239.52	50.26
Total Costs [$/day]		404.56	404.61	250.34
Energy [kWh/day]		7085.61	5454.60	5325.89
Peak Demand [kW]		591.05	1026.55	215.42
% Difference w.r.t. Case 0	Energy Costs	—	-38.09	-24.96
	Demand Charges	—	73.68	-63.55
	Total Costs	—	0.01	-38.12
	Energy	—	-23.02	-24.84
	Peak Demand	—	73.68	-63.55

† Monthly charges prorated per day.

TABLE III
COMPARISON OF LOAD CONTROL AND VOLTAGE OPTIMIZATION FOR WATER PUMPING FACILITY.

		Case 1	Case 2
Energy Costs [$/day]		186.86	200.51
Demand Charges† [$/day]		239.36	53.98
Total Costs [$/day]		426.22	254.49
Energy [kWh/day]		5477.36	5337.26
Peak Demand [kW]		1025.83	231.35
% Difference w.r.t. cases in Table II	Energy Costs	13.19	0.21
	Demand Charges	-0.07	7.39
	Total Costs	5.34	1.66
	Energy	0.42	0.21
	Peak Demand	-0.07	7.39

† Monthly charges prorated per day.

real-time control would be in the order 15-30 minutes [37], thus resulting in the need to solve the OILM model in less than 15-30 minutes, whenever the distribution feeder and customer operating conditions change significantly, which would be certainly feasible for all the case studies presented in the in the paper. For larger, more realistic distribution feeders, it is can be readily inferred from the results presented in [28] that the solution times should not exceed 15 minutes, thus allowing the proposed real-time application of the suggested approach in practice.

VI. CONCLUSIONS

This paper presented and discussed an optimal industrial load management (OILM) model, which can be readily integrated into EHMSs for the benefit of industrial customers and LDC system operators. The developed OILM model incorporates the modeling of processes, process interdependencies, storage units, distribution system components, and various other operating requirements set by distribution system and industrial process operators. The OILM model is generic and applicable to any industrial process, and its effectiveness is demonstrated through case studies carried out in two industrial processes, i.e., a flour mill and a water pumping facility. The results obtained from

the case studies show that the OILM model may yield significant savings to the industrial customers in energy prices and demand charges, and also help LDC system operators to reduce peak demand. Therefore, the proposed mathematical models, in conjunction with smart grid technologies at the customer and LDC levels, have certainly the potential to be beneficial to both industrial customers and LDC system operators.

Based on the encouraging results obtained from the simulations, we are right now in the process of validating these models through actual measurements in 3 different industrial facilities in Southern Ontario, Canada, including an Ontario Clean Water Agency (OCWA) water pumping facility. This has required collecting a large number of measurements over several months, so as to capture all the main aspects of the operations of the industrial loads being monitored and modeled. From preliminary results, to be fully reported in the future, the mathematical models described in the paper seem to be performing well.

Appendices

Only non-zero parameters used in the case studies of flour mill and water pumping facility are presented next.

A. Flour Mill Parameters

$$\Delta T = 1;\ \ T = 24;\ \ T_1 = 1;\ \ T_2 = 24$$
$$C = 4;\ \ J = 5$$

$$R_1 = [1];\ \ R_2 = \begin{bmatrix} 1 & 0 \\ 0 & 1 \end{bmatrix};\ \ R_3 = [0.8];\ \ R_4 = [1]$$

$$U' = \begin{bmatrix} 1 & 1 & 1 & 1 & 1 \end{bmatrix};\ \ D = \begin{bmatrix} 0 & 0 & 0 & 0 & 0 \\ 0 & 0 & 1 & 0 & 0 \\ 0 & 0 & 0 & 0 & 0 \\ 0 & 0 & 0 & 0 & 0 \\ 0 & 0 & 0 & 0 & 0 \end{bmatrix}$$

$$Pd_{1,t} = f_{1,t}(o_{1,1,t}) = 0.133\, o_{1,1,t}$$
$$Pd_{2,t} = f_{2,t}(o_{2,1,t}) = 11.043\, o_{2,1,t}$$
$$Pd_{3,t} = f_{3,t}(o_{3,1,t}) = 11.090\, o_{3,1,t}$$
$$Pd_{4,t} = f_{4,t}(o_{4,1,t}) = 36.650\, o_{4,1,t}$$
$$Pd_{5,t} = f_{5,t}(o_{5,1,t}) = 48.148\, o_{5,1,t}$$

$$O_{max} = \begin{bmatrix} 60.000 \text{ kl/h} \\ 2.330 \text{ tons/h} \\ 1.330 \text{ tons/h} \\ 1.660 \text{ tons/h} \\ 2.000 \text{ tons/h} \end{bmatrix};\ \ O_{min} = \begin{bmatrix} 30.000 \text{ kl/h} \\ 1.170 \text{ tons/h} \\ 0.665 \text{ tons/h} \\ 0.830 \text{ tons/h} \\ 1.000 \text{ tons/h} \end{bmatrix}$$

$$L_{cap} = \begin{bmatrix} \infty \\ 180 \text{ kl} \\ 0 \\ 6 \text{ tons} \end{bmatrix}$$

B. Water Pumping Facility Parameters

$$\Delta T = 1;\ \ T = 24;\ \ T_1 = 1;\ \ T_2 = 24$$
$$C = 2;\ \ J = 5$$
$$R_1 = R_2 = R_3 = R_4 = R_5 = [1]$$
$$V_{max} = 1.05 \times 4.16;\ \ V_{min} = 0.95 \times 4.16$$

$$O_{max} = \begin{bmatrix} 1800 \text{ m}^3\text{/h} \\ 1440 \text{ m}^3\text{/h} \\ 828 \text{ m}^3\text{/h} \\ 828 \text{ m}^3\text{/h} \\ 1800 \text{ m}^3\text{/h} \end{bmatrix};\ \ O_{min} = \begin{bmatrix} 900 \text{ m}^3\text{/h} \\ 720 \text{ m}^3\text{/h} \\ 414 \text{ m}^3\text{/h} \\ 414 \text{ m}^3\text{/h} \\ 900 \text{ m}^3\text{/h} \end{bmatrix}$$

$$L_0 = \begin{bmatrix} \infty \\ 7800 \text{ m}^3 \end{bmatrix};\ \ L_{min} = \begin{bmatrix} \infty \\ 2600 \text{ m}^3 \end{bmatrix}$$

$$L_{cap} = \begin{bmatrix} \infty \\ 18200 \text{ m}^3 \end{bmatrix};\ \ U' = \begin{bmatrix} 1 & 1 & 1 & 1 & 1 \end{bmatrix}$$

$$Pd_{1,t} = f_{1,t}(V_t, Q_{1,t}) = -476.633 + 0.527\, Q_{1,t} + 8.670\, V_t - 1.454 \times 10^{-4} Q_{1,t}^2 - 8.827\, V_t^2 + 1.257 \times 10^{-5}\, Q_{1,t}\, V_t$$
$$Pd_{2,t} = f_{2,t}(V_t, Q_{2,t}) = -356.480 + 0.492\, Q_{2,t} + 6.485\, V_t - 1.699 \times 10^{-4}\, Q_{2,t}^2 - 6.602\, V_t^2 + 1.175 \times 10^{-5}\, Q_{2,t}\, V_t$$
$$Pd_{3,t} = f_{3,t}(V_t, Q_{3,t}) = -59.448 + 0.140\, Q_{3,t} + 2.271\, V_t - 8.237 \times 10^{-5}\, Q_{3,t}^2 - 2.307\, V_t^2 + 5.817 \times 10^{-6}\, Q_{3,t}\, V_t$$
$$Pd_{4,t} = f_{4,t}(V_t, Q_{4,t}) = -59.448 + 0.140\, Q_{4,t} + 2.271\, V_t - 8.237 \times 10^{-5}\, Q_{4,t}^2 - 2.307\, V_t^2 + 5.817 \times 10^{-6}\, Q_{4,t}\, V_t$$
$$Pd_{5,t} = f_{5,t}(V_t, Q_{5,t}) = -476.633 + 0.527\, Q_{5,t} + 8.6703\, V_t - 1.454 \times 10^{-4} Q_{5,t}^2 - 8.827\, V_t^2 + 1.257 \times 10^{-5}\, Q_{5,t}\, V_t$$
$$Qd_{1,t} = g_{1,t}(V_t, Q_{1,t}) = 139.975 - 0.165\, Q_{1,t} + 6.741\, V_t + 4.873 \times 10^{-5}\, Q_{1,t}^2 - 6.876\, V_t^2 + 9.259 \times 10^{-6}\, Q_{1,t}\, V_t$$
$$Qd_{2,t} = g_{2,t}(V_t, Q_{2,t}) = 104.691 - 0.155\, Q_t + 5.042\, V_t + 5.695 \times 10^{-5}\, Q_{2,t}^2 - 5.143\, V_t^2 + 8.655 \times 10^{-6}\, Q_{2,t}\, V_t$$
$$Qd_{3,t} = g_{3,t}(V_t, Q_{3,t}) = 47.771 - 0.119\, Q_{3,t} + 0.819\, V_t + 7.421 \times 10^{-5}\, Q_{3,t}^2 - 0.849\, V_t^2 + 5.986 \times 10^{-6}\, Q_{3,t}\, V_t$$
$$Qd_{4,t} = g_{4,t}(V_t, Q_{4,t}) = 47.771 - 0.119\, Q_{4,t} + 0.819\, V_t + 7.420 \times 10^{-5}\, Q_{4,t} - 0.849\, V_t^2 + 5.986 \times 10^{-6}\, Q_{4,t}\, V_t$$
$$Qd_{5,t} = g_{5,t}(V_t, Q_{5,t}) = 139.975 - 0.165\, Q_{5,t} + 6.741\, V_t + 4.873 \times 10^{-5}\, Q_{5,t}^2 - 6.876\, V_t^2 + 9.259 \times 10^{-6}\, Q_{5,t}\, V_t$$

References

[1] A. Bose, "Smart Transmission Grid Applications and Their Supporting Infrastructure," *IEEE Trans. Smart Grid*, vol. 1, no. 1, pp. 11–19, Jun. 2010.

[2] "The Smart Grid: an Introduction." [Online]. Available: http://www.oe.energy.gov/DocumentsandMedia/DOE_SG_Book_Single_Pages.pdf

[3] R. Brown, "Impact of Smart Grid on Distribution System Design," in *Proc. IEEE PES General Meeting*, 2008, pp. 1–4.

[4] F. Goodman and M. McGranaghan, "EPRI Research Plan for Advanced Distribution Automation," in *Proc. IEEE PES General Meeting*, vol. 3, 2005, p. 2620.

[5] J. D. Kueck and B. J. Kirby, "Distribution System of the Future," Oak Ridge National Laboratory. [Online]. Available: http://www.ornl.gov/~webworks/cppr/y2001/rpt/116950.pdf

[6] G. T. Heydt, "The Next Generation of Power Distribution Systems," *IEEE Trans. Smart Grid*, vol. 1, no. 3, pp. 225–235, Dec. 2010.

[7] A. S. Bouhouras, G. T. Andreou, D. P. Labridis, and A. G. Bakirtzis, "Selective Automation Upgrade in Distribution Networks Towards a Smarter Grid," *IEEE Trans. Smart Grid*, vol. 1, no. 3, pp. 278 –285, Dec. 2010.
[8] A. P. S. Meliopoulos, G. Cokkinides, R. Huang, E. Farantatos, S. Choi, Y. Lee, and X. Yu, "Smart Grid Technologies for Autonomous Operation and Control," *IEEE Trans. Smart Grid*, vol. 2, no. 1, pp. 1–10, Mar. 2011.
[9] M. Geidl, G. Koeppel, P. Favre-Perrod, B. Klöckl, G. Andersson, and K. Fröhlich, "Energy Hubs for the Future," *IEEE Power and Energy Magazine*, vol. 5, no. 1, pp. 24–30, Jan.-Feb. 2007.
[10] lM. Schulze, L. Friedrich, and M. Gautschi, "Modeling and Optimization of Renewables: Applying the Energy Hub Approach," in *Proc. IEEE International Conference Sustainable Energy Technologies*, Nov. 2008, pp. 83–88.
[11] T. Krause, G. Andersson, K. Fröhlich, and A. Vaccaro, "Multiple-Energy Carriers: Modeling of Production,Delivery, and Consumption," *Proc. of the IEEE*, vol. 99, no. 1, pp. 15 –27, Jan. 2011.
[12] M. C. Bozchalui, S. A. Hashmi, H. Hassen, C. A. Cañizares, and K. Bhattacharya, "Optimal Operation of Residential Energy Hubs in Smart Grids," *IEEE Trans. Smart Grid*, vol. 3, no. 4, pp. 1755 –1766, Dec. 2012.
[13] "The Energy Hub Management System: Enabling and Empowering Energy Managers Through Increased Information and Control," University of Waterloo. [Online]. Available: http://www.energyhub.uwaterloo.ca/
[14] X. Guan, Z. Xu, and Q.-S. Jia, "Energy-Efficient Buildings Facilitated by Microgrid," *IEEE Trans. Smart Grid*, vol. 1, no. 3, pp. 243–252, Dec. 2010.
[15] A. Molderink, V. Bakker, M. G. C. Bosman, J. L. Hurink, and G. J. M. Smit, "Management and Control of Domestic Smart Grid Technology," *IEEE Trans. Smart Grid*, vol. 1, no. 2, pp. 109–119, Sep. 2010.
[16] M. A. A. Pedrasa, T. D. Spooner, and I. F. MacGill, "Coordinated Scheduling of Residential Distributed Energy Resources to Optimize Smart Home Energy Services," *IEEE Trans. Smart Grid*, vol. 1, no. 2, pp. 134–143, Sep. 2010.
[17] E. T. Jauch, "'Conservation Biased' Distribution Volt/Var/(kW) Management," in *Proc. IEEE PES General Meeting*, 2009, pp. 1–7.
[18] R. W. Beck, "Distribution Efficiency Initiative," Northwest Energy Alliance, Dec. 2007. [Online]. Available: www.rwbeck.com/neea.pdf
[19] T. Wilson, K. Benson, and D. Bell, "Saving Megawatts with Voltage Optimization," PCS Utilidata. [Online]. Available: http://utilidata.com/userfiles/file/Industrial%20Voltage%20Optimization.pdf
[20] A. I. Cohen and C. C. Wang, "An Optimization Method for Load Management Scheduling," *IEEE Trans. Power Syst.*, vol. 3, no. 2, pp. 612–618, May 1988.
[21] C. O. Bjork and B. G. Karlsson, "Load Management Applications for Industrial Loads," *IEEE Trans. Power App. Syst.*, vol. PAS-104, no. 8, pp. 2058–2063, Aug. 1985.
[22] "Electrical Power Systems and Equipments-Voltage Ratings," ANSI Standard C 84.1-1995.
[23] B. Baran, C. V. Lucken, and A. Sotelo, "Multi-objective Pump Scheduling Optimisation Using Evolutionary Strategies," *Journals of Advances in Engineering Software*, vol. 36, no. 1, pp. 39–47, 2005.
[24] S. Ashok and R. Banerjee, "An Optimization Mode for Industrial Load Management," *IEEE Trans. Power Syst.*, vol. 16, no. 4, pp. 879–884, Nov. 2001.
[25] S. Ashok and R. Banerjee, "Optimal Operation of Industrial Cogeneration for Load Management," *IEEE Trans. Power Syst.*, vol. 18, no. 2, pp. 931–937, May 2003.
[26] V Chandan, A.-T. Do, J. Baoduo, F. Jabbari, J. Brouwer, I. Akrotirianakis, A. Chakraborty, and A. Alleyne, "Modeling and Optimization of a Combined Cooling, Heating and Power Plant System," in *Proc. American Control Conference*, Jun. 2012, pp. 3069-3074.
[27] S. Paudyal, "Optimal Operation of Distribution Systems and Industrial Energy Hubs in Smart Grids," PhD Thesis, University of Waterloo, Department of Electrical and Computer Engineering, 2012.
[28] S. Paudyal, C. A. Cañizares, and K. Bhattacharya, "Optimal Operation of Distribution Feeders in Smart Grids," *IEEE Trans. Ind. Electron.*, vol. 58, no. 10, pp. 4495–4503, Oct. 2011.
[29] W. H. Kersting, *Distribution System Modeling and Analysis*, 2nd ed. Boca Raton: CRC Press, 2006.
[30] W. H. Kersting, "Radial Distribution Test Feeders," in *Proc. IEEE PES Winter Meeting*, vol. 2, 2001, pp. 908–912.
[31] N. R. Draper and H. Smith, *Applied Regression Analysis*, 3rd ed. New York: Wiley, 1998.
[32] "GAMS Release 2.25," A Users Guide, GAMS Development Corporation, 1998.
[33] "KNITRO 6.0," User's Manual, Ziena Optimization Inc., 2009.
[34] "A Guide to Electricity Charges-Market Participants." [Online]. Available: http://www.ieso.ca/imoweb/role/wholesaleCharges.asp
[35] "A Guide to Electricity Charges for Business." [Online]. Available: http://www.ieso.ca/imoweb/siteshared/electricity_charges.asp
[36] "PSCAD," Manitoba-HVDC Research Centre. [Online]. Available: https://pscad.com/
[37] S. Paudyal, C. A. Cañizares, and K. Bhattacharya, "Three-phase Distribution OPF in Smart Grids: Optimality versus Computational Burden," in *proc. IEEE PES Innovative Smart Grid Technologies*, Dec. 2011, pp. 1-7.



Sumit Paudyal (S'07, M'13) received the Bachelor's degree in Electrical Engineering from Tribhuvan University, Kathmandu, Nepal, in 2003, the M.Sc. degree in Electrical Engineering from the University of Saskatchewan, SK, Canada, in 2008, and the Ph.D. degree in Electrical Engineering at the University of Waterloo, Waterloo, ON, Canada in 2012. He joined the Department of ECE, Michigan Technological University, Houghton, MI, USA, as an Assistant Professor in 2012. He was a Research Assistant with Kathmandu Engineering College in 2003 and an Electrical Engineer with the Nepal Electricity Authority in 2004. His research interests include Smart Distribution Grid Operations, Power System Protection, Power System Real-time Hardware Simulations, and Optimization Techniques in Power Systems.



Claudio A. Cañizares (S'86, M'91, SM'00, F'07) received the electrical engineer diploma from the Escuela Politécnica Nacional (EPN), Quito, Ecuador, in 1984 and the M.S. and Ph.D. degrees electrical engineering are from the University of Wisconsin-Madison in 1988 and 1991, respectively. He has held various academic and administrative positions at the Electrical and Computer Engineering Department of the University of Waterloo, Waterloo, ON, Canada, since 1993, where he is currently a full Professor and the Associate Director of the Waterloo Institute for Sustainable Energy (WISE). He was awarded the Hydro One research chair in 2010. His research activities concentrate in the study of stability, modeling, simulation, control, and computational issues in power systems within the context of competitive electricity markets and smart grids.

Dr. Cañizares has been the recipient of various IEEE-PES Working Group awards and holds and has held several leadership appointments in IEEE-PES technical committees and subcommittees. He is a Fellow of the Royal Society of Canada in 2012, and is a Registered Professional Engineer in the province of Ontario since 1995.



Kankar Bhattacharya (M'95, SM'01) received the Ph.D. degree in Electrical Engineering from the Indian Institute of Technology, New Delhi, India in 1993. He was in the faculty of Indira Gandhi Institute of Development Research, Mumbai, India, during 1993-1998, and then the Department of Electric Power Engineering, Chalmers University of Technology, Gothenburg, Sweden, during 1998-2002. He joined the E&CE Department of the University of Waterloo, Canada, in 2003 where he is currently a full Professor. His research interests are in power system economics and operational aspects.